

Renal phenotype in mice lacking the Kir5.1 (*Kcnj16*) K⁺ channel subunit contrasts with that observed in SeSAME/EAST syndrome

Marc Paulais^{a,b,1}, May Bloch-Faure^{a,b}, Nicolas Picard^{a,b}, Thibaut Jacques^{b,c}, Suresh Krishna Ramakrishnan^{a,b}, Mathilde Keck^{a,b}, Fabien Sohet^{a,b}, Dominique Eladari^{a,b,c,d}, Pascal Houillier^{a,b,c,d}, Stéphane Lourdel^{a,b}, Jacques Teulon^{a,b}, and Stephen J. Tucker^e

^aUniversité Pierre et Marie Curie Paris 6, Université Paris 5, and Institut National de la Santé et de la Recherche Médicale, Unité Mixte de Recherche en Santé 872, 75006 Paris, France; ^bCentre National de la Recherche Scientifique, Équipes de Recherche Labellisées 7226, Genomics Physiology, and Renal Physiopathology Laboratory, Centre de Recherche des Cordeliers, 75270 Paris 6, France; ^cFaculty of Medicine, Université Paris-Descartes, 75006 Paris, France; ^dAssistance Publique-Hôpitaux de Paris, Hôpital Européen Georges Pompidou, 75015 Paris, France; and ^eClarendon Laboratory and Department of Physics, University of Oxford, Oxford OX1 3PU, United Kingdom

Edited by Maurice B. Burg, National Heart, Lung, and Blood Institute, Bethesda, MD, and approved May 9, 2011 (received for review January 31, 2011)

The heteromeric inwardly rectifying Kir4.1/Kir5.1 K⁺ channel underlies the basolateral K⁺ conductance in the distal nephron and is extremely sensitive to inhibition by intracellular pH. The functional importance of Kir4.1/Kir5.1 in renal ion transport has recently been highlighted by mutations in the human Kir4.1 gene (*KCNJ10*) that result in seizures, sensorineural deafness, ataxia, mental retardation, and electrolyte imbalance (SeSAME)/epilepsy, ataxia, sensorineural deafness, and renal tubulopathy (EAST) syndrome, a complex disorder that includes salt wasting and hypokalemic alkalosis. Here, we investigated the role of the Kir5.1 subunit in mice with a targeted disruption of the Kir5.1 gene (*Kcnj16*). The *Kir5.1*^{-/-} mice displayed hypokalemic, hyperchloremic metabolic acidosis with hypercalciuria. The short-term responses to hydrochlorothiazide, an inhibitor of ion transport in the distal convoluted tubule (DCT), were also exaggerated, indicating excessive renal Na⁺ absorption in this segment. Furthermore, chronic treatment with hydrochlorothiazide normalized urinary excretion of Na⁺ and Ca²⁺, and abolished acidosis in *Kir5.1*^{-/-} mice. Finally, in contrast to WT mice, electrophysiological recording of K⁺ channels in the DCT basolateral membrane of *Kir5.1*^{-/-} mice revealed that, even though Kir5.1 is absent, there is an increased K⁺ conductance caused by the decreased pH sensitivity of the remaining homomeric Kir4.1 channels. In conclusion, disruption of *Kcnj16* induces a severe renal phenotype that, apart from hypokalemia, is the opposite of the phenotype seen in SeSAME/EAST syndrome. These results highlight the important role that Kir5.1 plays as a pH-sensitive regulator of salt transport in the DCT, and the implication of these results for the correct genetic diagnosis of renal tubulopathies is discussed.

kidney | homeostasis | acid–base balance

K⁺ channels play critical roles in renal tubular transport functions directly by providing a secretory pathway for K⁺ or indirectly by controlling membrane voltage and K⁺ recycling across the plasma membrane (1). Recent genetic and functional studies have shown that loss of renal K⁺ channel activity not only has an impact on K⁺ balance, but also affects other ion transport systems and the regulation of the acid–base balance. For instance, it has been clearly established that inherited mutations of the human *KCNJ1* gene underlie type II Bartter syndrome, a severe disorder involving renal salt wasting and hypokalemic metabolic alkalosis (2). Likewise, inactivation of the *Kcnk5* gene encoding the acid- and volume-sensitive TASK2 K⁺ channel induces renal HCO₃⁻ loss and metabolic acidosis in mice (3).

The cortical thick ascending limb (4, 5), distal convoluted tubule (DCT) (6, 7), and cortical collecting duct (CCD) principal cells (8, 9) are endowed with K⁺ channels displaying properties identical to inwardly rectifying heteromeric Kir4.1/Kir5.1 K⁺ channels (10). Recent studies have reported that rare homozygous missense mutations of the human *KCNJ10* gene, which

encodes the Kir4.1 subunit, underlie SeSAME/EAST syndrome, a rare disorder in which patients experience neurological and renal symptoms (11, 12). In the kidney, it is thought that these loss-of-function mutations in Kir4.1 impair the function of heteromeric Kir4.1/Kir5.1 channels (13, 14), thereby dramatically impairing salt reuptake from the DCT, and increasing downstream K⁺ and H⁺ secretion. This results in a Gitelman-like syndrome, characterized by salt wasting, hypocalciuria, hypomagnesaemia, and hypokalemic metabolic alkalosis (11, 12, 15).

The basolateral location of Kir4.1/Kir5.1 channels obviously suggests a role for these channels in maintenance of the basolateral membrane potential, and in the “recycling” across the basolateral membrane of any K⁺ that enters the cell via the basolateral Na⁺/K⁺ ATPase. The recycling of K⁺ is a crucial step for sustained transepithelial Na⁺ reabsorption. However, in the DCT of patients with seizures, sensorineural deafness, ataxia, mental retardation, and electrolyte imbalance (SeSAME)/epilepsy, ataxia, sensorineural deafness, and renal tubulopathy (EAST) syndrome, this K⁺ recycling seems to be altered.

The expression of Kir5.1 alone does not produce detectable K⁺ currents in most recombinant expression systems (16). Instead, this “silent” subunit appears to heteromultimerize with Kir4.1 to produce novel Kir4.1/Kir5.1 channels (17–19) that have an extreme sensitivity to intracellular pH (pH_i) within the physiological range (i.e., pK_a of 7.4) (18, 20, 21). By contrast, homomeric Kir4.1 channels are only mildly sensitive to pH_i (pK_a, 6.0). This therefore raises the important question of how Kir5.1 contributes to renal ion transport and the role of these highly pH-sensitive Kir4.1/Kir5.1 channels in this process.

The present study addresses this issue by using a recently created strain of mice in which the Kir5.1 (*Kcnj16*) gene has been deleted (22). We show that deletion of this subunit results in a pH_i-insensitive, highly active K⁺ conductance in the DCT basolateral membrane, and a severe renal phenotype characterized by hypokalemic metabolic acidosis with hypercalciuria. Thus, instead of producing an effect similar to SeSAME/EAST syndrome mutations in Kir4.1, inactivation of Kir5.1 reduces the pH_i sensitivity of the DCT basolateral K⁺ conductance and produces a mirror-image phenotype to SeSAME/EAST syndrome by increasing the mean basolateral K⁺ conductance in the distal nephron.

Author contributions: M.P. and J.T. designed research; M.P., M.B.-F., N.P., T.J., S.K.R., M.K., F.S., P.H., S.L., and J.T. performed research; M.P., N.P., T.J., S.L., and J.T. analyzed data; and M.P., D.E., J.T., and S.J.T. wrote the paper.

The authors declare no conflict of interest.

This article is a PNAS Direct Submission.

¹To whom correspondence should be addressed. E-mail: marc.paulais@crc.jussieu.fr.

This article contains supporting information online at www.pnas.org/lookup/suppl/doi:10.1073/pnas.1101400108/-DCSupplemental.

Results

Clinical Parameters of *Kir5.1*^{-/-} Mice. There was no obvious difference in the survival or gross physical appearance between *Kir5.1*^{+/+} and *Kir5.1*^{-/-} mice maintained on a control diet, except for an approximately 15% lower body weight of the *Kir5.1*^{-/-} mice ($P < 0.0001$; Table 1). *Kir5.1*^{-/-} mice were slightly polydipsic, and exhibited polyuria and correspondingly lower urine osmolality. However, both groups of mice adapted normally to 24 h water restriction (Fig. 1), indicating that the urine-concentrating ability of *Kir5.1*^{-/-} mice is not impaired. Furthermore, the hematocrit level of *Kir5.1*^{-/-} mice was not increased ($45.7 \pm 1.42\%$ vs. $45.5 \pm 1.13\%$ for *Kir5.1*^{+/+} and *Kir5.1*^{-/-} mice, respectively; $P = 0.4$), indicating the absence of dehydration.

***Kir5.1*^{-/-} Mice Display Metabolic Acidosis and Hypokalemia.** Blood and plasma analyses revealed that *Kir5.1*^{-/-} mice had metabolic hyperchloremic acidosis (Table 1). However, despite this acidosis, urinary NH_4^+ excretion was not increased (81 ± 3.5 mmol/mmol creatinine in 10 *Kir5.1*^{-/-} mice vs. 99 ± 5.2 mmol/mmol creatinine in 11 *Kir5.1*^{+/+} mice). Also, glomerular filtration rates were similar in *Kir5.1*^{+/+} mice (308 ± 43 $\mu\text{L}/\text{min}$; $n = 11$) and *Kir5.1*^{-/-} mice (272 ± 35 $\mu\text{L}/\text{min}$; $n = 7$; $P = 0.54$), indicating the absence of chronic renal failure. Our data therefore clearly show that *Kir5.1*^{-/-} mice have renal tubular acidosis. However, this may also be associated with a respiratory component because the *Kir5.1*^{-/-} mice do not display the expected compensatory decrease in blood P_{CO_2} (Table 1), an effect that would be consistent with the respiratory phenotype recently reported in these mice (22).

In addition to renal acidosis, the *Kir5.1*^{-/-} mice also exhibited hypokalemia, associated with increased renal K^+ excretion, as well as hypercalciuria and hypermagnesuria (Table 1). However, *Kir5.1*^{-/-} mice were able to balance Na^+ normally, and had normal blood pressure and 24-h urinary aldosterone excretion rates (Table 1).

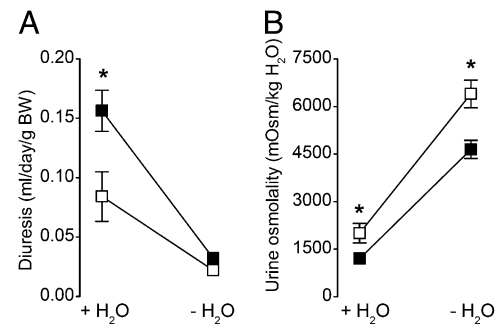


Fig. 1. Urine-concentrating ability of *Kir5.1*^{+/+} and *Kir5.1*^{-/-} mice. Daily diuresis (A) and urine osmolality (B) of *Kir5.1*^{+/+} (□) and *Kir5.1*^{-/-} (■) mice maintained in metabolic cages were first measured while the mice had free access to demineralized water (+H₂O), and then after a 24-h period of water deprivation (-H₂O). Weight loss induced by water deprivation averaged 7% and 9% for *Kir5.1*^{+/+} and *Kir5.1*^{-/-} mice, respectively. Water deprivation tests showed that both groups of mice had similar urine-concentrating abilities. Values are mean values for 10 *Kir5.1*^{+/+} and eight *Kir5.1*^{-/-} mice. Error bars represent SEM when larger than symbols. * $P < 0.05$, *Kir5.1*^{-/-} versus *Kir5.1*^{+/+} mice.

No Alteration in the Responses to Furosemide and Amiloride in *Kir5.1*^{-/-} Mice. Expression of Kir5.1 is also seen in the TAL and DCT cells, as well as in CCD principal cells, where it coassembles with Kir4.1 to form Kir4.1/Kir5.1 channels in the basolateral membrane (5, 6, 9). We therefore investigated the effects of *Kcnj16* disruption on NaCl transport in vivo by monitoring the response to diuretics in these nephron segments. TAL function was challenged with the loop diuretic furosemide, an inhibitor of the apical $\text{Na}^+-\text{K}^+-2\text{Cl}^-$ cotransporter. Fig. 2A shows that *Kir5.1*^{+/+} ($n = 12$) and *Kir5.1*^{-/-} mice ($n = 12$) responded with similar increases in the urinary excretion of Na^+ and Ca^{2+} 6 h

Table 1. Biological parameters in *Kir5.1*^{+/+} and *Kir5.1*^{-/-} mice

Parameter	<i>Kir5.1</i> ^{+/+} ($n = 11$)	<i>Kir5.1</i> ^{-/-} ($n = 10$)
Total BW, g	27.9 \pm 0.26	24.7 \pm 0.57*
Water intake, $\mu\text{L}/\text{g}$ BW/d	167 \pm 16	228 \pm 14 [†]
Systolic blood pressure, mm Hg	109.8 \pm 2.4	104 \pm 2.6
Urine		
Uv, $\mu\text{L}/\text{g}$ BW/d	52 \pm 11	105 \pm 14 [†]
Osmolality, mOsm/kg H ₂ O	2598 \pm 247	1718 \pm 167 [†]
pH	5.62 \pm 0.04	5.68 \pm 0.04
Na^+ , mmol/mmol creatinine	75.3 \pm 4.8	67.6 \pm 2.7
K^+ , mmol/mmol creatinine	8.23 \pm 1.45	14.36 \pm 1.77 [‡]
Cl^- , mmol/mmol creatinine	137.4 \pm 10.2	136 \pm 5.6
Ca^{2+} , mmol/mmol creatinine	0.43 \pm 0.06	1.82 \pm 0.35 [‡]
Mg^{2+} , mmol/mmol creatinine	2.68 \pm 0.25	3.42 \pm 0.2 [§]
Aldosterone, $\mu\text{mol}/\text{mmol}$ creatinine	3.38 \pm 0.54	2.71 \pm 0.4
Blood		
pH	7.35 \pm 0.015	7.19 \pm 0.015*
PCO_2 , mm Hg	45.5 \pm 1.1	45.7 \pm 1.4
$[\text{HCO}_3^-]$, mM	24.4 \pm 0.5	16.9 \pm 0.3*
Plasma		
Osmolality (mOsm/kg H ₂ O)	305 \pm 1.7	303 \pm 5.2
$[\text{Cl}^-]$, mM	122.5 \pm 0.7	130.6 \pm 0.8*
$[\text{Na}^+]$, mM	149.8 \pm 2.4	153.1 \pm 0.5
$[\text{K}^+]$, mM	4.4 \pm 0.14	3.9 \pm 0.12 [‡]
$[\text{Ca}^{2+}]$, mM	1.26 \pm 0.007	1.27 \pm 0.009
$[\text{Mg}^{2+}]$, mM	1.66 \pm 0.15	1.53 \pm 0.37

Values are mean \pm SEM for the numbers of animals given in brackets, except for fractional excretions in *Kir5.1*^{-/-} mice, where $n = 7$, for plasma K^+ concentration of *Kir5.1*^{+/+} and *Kir5.1*^{-/-} mice, where $n = 9$ and $n = 6$, respectively, and for diastolic blood pressure of *Kir5.1*^{+/+} mice, where $n = 12$.

* $P < 0.0001$, [†] $P < 0.005$, [‡] $P < 0.05$, and [§] $P < 0.01$.

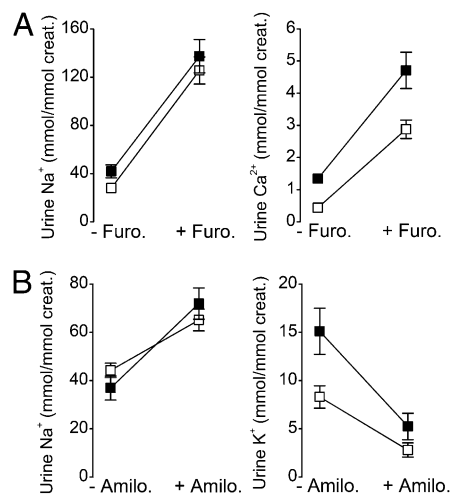


Fig. 2. Effects of furosemide and amiloride. *Kir5.1*^{+/+} (□) and *Kir5.1*^{-/-} (■) mice maintained in metabolic cages were subjected to furosemide (A) or amiloride (B) treatment for 6 h. Urinary Na⁺ and Ca²⁺ excretion were measured before (-Furo) and after (+Furo) furosemide treatment, and urinary Na⁺ and K⁺ excretion were measured before (-Amilo) and after (+Amilo) amiloride treatments. Values are means for 12 (A) or 10 (B) *Kir5.1*^{+/+} mice and 12 (A) or eight (B) *Kir5.1*^{-/-} mice. Error bars represent SEM when larger than symbols. All diuretic-induced responses were statistically significant ($P < 0.05$).

after start of the treatment. Administration of the diuretic also similarly increased urine volume and urinary K⁺ and Mg²⁺ excretion (Table S1). Thus, NaCl absorption in the TAL is clearly not affected in *Kir5.1*^{-/-} mice.

We next investigated the effects of the K⁺-sparing diuretic amiloride, a blocker of the apical epithelial sodium channel (ENaC), which mediates sodium absorption in the aldosterone-sensitive distal nephron (ASDN). As expected, amiloride (Fig. 2B) increased urinary Na⁺ while decreasing urinary K⁺ excretion 6 h after its injection. However, the response to amiloride was the same in both groups of mice, indicating that ENaC-mediated Na⁺ absorption is not altered by deletion of *Kir5.1*.

Increased Response to Hydrochlorothiazide in *Kir5.1*^{-/-} Mice. Loss of function mutations in *Kir4.1* predominantly affect DCT ion transport (11, 12). We therefore investigated the effects of hydrochlorothiazide (HCTZ), an inhibitor of the apical NaCl cotransporter in the DCT. Six hours after a single HCTZ injection, similar diuretic responses were observed in *Kir5.1*^{+/+} and *Kir5.1*^{-/-} mice, with 3.5-fold increases in urine volume, and parallel increases in the excretion of K⁺ and Mg²⁺ (Table S2). However, as shown in Fig. 3A, HCTZ induced a significantly greater increase in Na⁺ urine excretion in *Kir5.1*^{-/-} mice than in *Kir5.1*^{+/+} mice. HCTZ administration also normalized calciuria in *Kir5.1*^{-/-} mice. These findings therefore demonstrate that genetic inactivation of *Kir5.1* stimulates salt absorption in the DCT.

Interestingly, in type II pseudohypoaldosteronism (PHAII), WNK4 mutant mice also exhibit renal acidosis and hypercalciuria, an effect thought to be caused by excessive NaCl absorption in the DCT. This effect can also be corrected in the presence of thiazide (23, 24), and patients with PHAII are known to be highly sensitive to thiazide therapy (25, 26). This therefore prompted us to test the effects of chronic HCTZ treatment on *Kir5.1*^{+/+} and *Kir5.1*^{-/-} mice. Interestingly, after treatment with HCTZ for 4 d, we observed a significant increase in blood pH and bicarbonate, showing that HCTZ abolished metabolic acidosis (Table 2). However, the effects of HCTZ treatment on urinary Ca²⁺ excretion were the same in both groups of mice ($P = 0.37$; Fig. 3B).

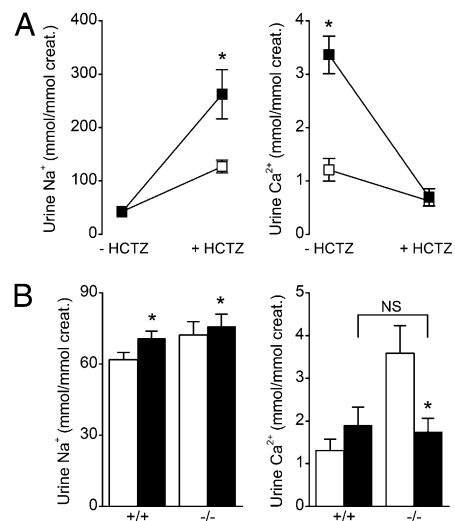


Fig. 3. Short- and long-term effects of HCTZ. (A) Urinary Na⁺ and Ca²⁺ excretion of *Kir5.1*^{+/+} (□) and *Kir5.1*^{-/-} (■) mice were measured before (-HCTZ) and after 6 h of treatment (+HCTZ). (B) Urinary Na⁺ (Left) and Ca²⁺ (Right) were measured in *Kir5.1*^{+/+} and *Kir5.1*^{-/-} mice before (white bars) and after (black bars) a 4-d HCTZ treatment. Values are means \pm SEM for 10 (A) or 12 (B) *Kir5.1*^{+/+} mice and nine (A) or 12 (B) *Kir5.1*^{-/-} mice. * $P < 0.05$ versus control; NS, no significant difference at $P < 0.05$.

Expression of Transport Proteins. According to our findings, *Kir5.1*^{-/-} mice do not display a global sodium imbalance, even though salt transport is increased in their DCT. We therefore determined the relative levels of protein expression for a range of key transport proteins as an indirect measurement of their ion transport capacities in the proximal convoluted tubule, TAL, DCT, and ASDN. However, there was no difference in levels of expression for the NHE3 Na⁺/H⁺ exchanger, the Na⁺-K⁺-2Cl⁻ (NKCC2) and Na⁺-Cl⁻ (NCC) cotransporters, or the ENaC α -subunit (α ENaC) between the two groups of mice (Fig. S1), indicating that the alteration of transport we observe probably depends on changes in regulation rather than on differences in the maximal transport capacity per se.

Distinct K⁺ Channels in the DCT Basolateral Membranes of *Kir5.1*^{+/+} and *Kir5.1*^{-/-} Mice. In the DCT, the basolateral K⁺ channel has been shown to be a heteromeric *Kir4.1/Kir5.1* channel (6). Therefore, the loss-of-function mutations in *Kir4.1* associated with SeSAME/EAST syndrome are predicted to reduce the functional activity of this basolateral K⁺ channel (13, 14, 27). However, the functional properties of heteromeric *Kir4.1/Kir5.1* channels

Table 2. Long-term effects of HCTZ on plasma and blood parameters of *Kir5.1*^{+/+} and *Kir5.1*^{-/-} mice

Parameter	<i>Kir5.1</i> ^{+/+}		<i>Kir5.1</i> ^{-/-}	
	-HCTZ	+HCTZ	-HCTZ	+HCTZ
pH	7.24 \pm 0.03	7.30 \pm 0.02	7.09 \pm 0.05	7.22 \pm 0.04*
PCO ₂ , mm Hg	59.3 \pm 2.5	56 \pm 1.1	56.4 \pm 2.64	55.6 \pm 1.92
[HCO ₃ ⁻], mM	23.7 \pm 1.8	27.3 \pm 1*	16.9 \pm 1.4	22.3 \pm 1.2 [†]
[Cl ⁻], mM	119 \pm 1	113 \pm 0.3 [†]	126 \pm 1.27	114 \pm 0.96 [†]
[Na ⁺], mM	153.7 \pm 2.7	151.2 \pm 1.29	156.2 \pm 1.86	151 \pm 1.76
[Ca ²⁺], mM	1.21 \pm 0.02	1.16 \pm 0.03	1.17 \pm 0.03	1.15 \pm 0.02

Parameters were determined from retroorbital blood samples taken before and after a 4-d treatment with HCTZ. Values are means \pm SEM, for 11 *Kir5.1*^{+/+} and 12 *Kir5.1*^{-/-} mice.

* $P < 0.05$ and [†] $P = 0.0005$, Wilcoxon signed-rank test.

DCT function was stimulated in *Kir5.1*^{-/-} mice. Thus, apart from the presence of hypokalemia, the phenotype observed in these mice is the reverse of that seen in neonatal *Kcnj10* KO mice (11), and a mirror image of that seen in SeSAME/EAST syndrome.

Enhanced NCC activity is also the mark of PHAI, which includes metabolic acidosis and hypercalciuria, but is mainly characterized by hypertension, low aldosterone level, and hypokalemia (23–26). HCTZ reverses all the abnormalities in patients with PHAI (26), suggesting that K⁺ and H⁺ secretion by the distal nephron is down-regulated in this disease. In contrast, chronic treatment of *Kir5.1*^{-/-} mice with HCTZ rectified the metabolic acidosis and hypercalciuria, but not the hyperkalemia. In addition, ENaC-mediated Na⁺ absorption in the ASDN seems to be normal. This suggests that the metabolic acidosis and hypokalemia seen in *Kir5.1*^{-/-} mice might have another, nondistal, origin. Nijenhuis et al. (33) postulated that a compensatory increase in Na⁺ absorption by the proximal tubule occurs during NCC inhibition, thus increasing passive Ca²⁺ absorption in this segment, a hypothesis also put forward by Bockenhauer et al. (11) for patients affected by EAST syndrome. Conversely, it has also been suggested that the metabolic acidosis in PHAI patients may be a result of reduced bicarbonate absorption and ammonia production in the proximal tubule (34). In the present study, the low urinary pH and low NH₄⁺ excretion rate in *Kir5.1*^{-/-} mice would be compatible with a down-regulated proximal tubule absorption.

Recombinant heteromeric Kir4.1/Kir5.1 and homomeric Kir4.1 channels display distinct properties in terms of their single-channel conductance (40–60 vs. 20 pS) (10, 16, 18, 21), P_o (~0.4 vs. ~0.9 at pH_i 7.4) (21), and, in particular, their sensitivity to pH_i. This has enabled their identification in several native tissues, e.g., Kir4.1-like channels have been identified in native retinal Müller cells (31, 35) and retinal pigment epithelium (30), whereas heteromeric Kir4.1/Kir5.1-like channels have been proposed to resemble those found in the basolateral membrane of epithelia in the distal nephron (5, 6, 9). Therefore, our results provide further direct confirmation that the basolateral K⁺ conductance in the DCT is indeed produced by heteromeric Kir4.1/Kir5.1 channels.

Taken together, recent reports on SeSAME/EAST syndrome (11, 12) and the findings we report here show that DCT salt absorption can be dramatically altered by changes in Kir4.1/Kir5.1 K⁺ channel activity. Although the mechanisms involved remain elusive, a possible explanation may be found within the framework of the long-lived “pump and K⁺ conductance coupling” hypothesis (36–38). Transepithelial salt transport occurs according to a generally accepted model (Fig. 5A) in which the Na⁺/K⁺-ATPase maintains a favorable electrochemical gradient for Na⁺ influx at the apical membrane and provides an exit pathway for Na⁺ at the basolateral membrane. However, the continued functioning of Na⁺/K⁺-ATPase requires that K⁺ entering the cell via the Na⁺/K⁺-ATPase be recycled across the basolateral membrane via K⁺ channels. Accordingly, a decrease in basolateral K⁺ conductance would be expected to reduce transepithelial salt absorption, as observed in SeSAME/EAST syndrome, whereas an increase would up-regulate it (Fig. 5B), as we observe here with our *Kir5.1*^{-/-} mice. In this regard, the fact that the phenotypic effects of disrupting the *Kcnj10* or *Kcnj16* genes are mainly observed in the DCT and not the TAL and CCD is consistent with our previous observations, which showed that Kir4.1/Kir5.1 is the only K⁺ channel species present in DCT basolateral membrane (39), whereas the TAL and CCD principal cells are endowed with additional basolateral K⁺ channels (9, 39).

Interestingly, the pH_i sensitivity of the DCT basolateral K⁺ conductance appears to be a key regulatory factor. Although homomeric Kir4.1 channels exhibit a mild sensitivity to inhibition by pH_i (pK_a, 6.0–6.4), heteromultimerization with Kir5.1 dramatically increases this pH_i sensitivity and shifts it into the physiological range (pK_a, 7.1–7.4) (10, 19–21, 29). The significant increase in pH sensitivity conferred by Kir5.1 means that, for

Figure 5 consists of two diagrams, A and B, illustrating a cellular model for enhanced salt transport in the distal convoluted tubule (DCT). Both diagrams show a cell with an apical membrane facing the lumen and a basolateral membrane facing the interstitium. In diagram A, the cell contains an NCC (Na⁺/Cl⁻ cotransporter) on the apical membrane, a Na⁺/K⁺ ATPase pump on the basolateral membrane, and Kir4.1/Kir5.1 channels on the basolateral membrane. The Na⁺/K⁺ ATPase pump moves 3 Na⁺ ions out and 2 K⁺ ions in. The Kir4.1/Kir5.1 channels allow K⁺ to exit the cell. A dashed arrow indicates that pH_i (intracellular pH) is sensed by the Kir4.1/Kir5.1 channels. In diagram B, the cell contains an NCC on the apical membrane, a Na⁺/K⁺ ATPase pump on the basolateral membrane, and Kir4.1 channels on the basolateral membrane. The Na⁺/K⁺ ATPase pump moves 3 Na⁺ ions out and 2 K⁺ ions in. The Kir4.1 channels allow K⁺ to exit the cell. A dashed arrow indicates that pH_i is sensed by the Kir4.1 channels. The diagrams also show Cl⁻ ions being transported out of the cell through CIC-Kb channels on the basolateral membrane. The overall effect is an increase in salt reabsorption.

Fig. 5. A cellular model for enhanced salt transport in DCT caused by deletion of *Kcnj16*. (A) Basolateral Kir4.1/Kir5.1 channels recycle K⁺ entering the cell via the Na⁺/K⁺ ATPase. The continuous functioning of the Na⁺/K⁺ ATPase maintains a chemical gradient favorable to Na⁺ and Cl⁻ apical entry via the thiazide-sensitive electroneutral NCC. Kir4.1/Kir5.1 channels also maintain a negative basolateral membrane potential difference, thus providing a favorable electrochemical gradient to basolateral Cl⁻ exit through CIC-Kb Cl⁻ channels. Changes in pH_i are sensed by Kir4.1/Kir5.1 channels and affect basolateral K⁺ conductance, thereby modulating salt reabsorption by DCT cells. (B) *Kcnj16* deletion induces the formation of pH_i-insensitive and constitutively highly active basolateral homomeric Kir4.1 channels. The resulting increase in basolateral K⁺ conductance is expected to enhance basolateral Cl⁻ exit and Na⁺-K⁺ ATPase and NCC transport activities and thus to up-regulate overall salt reabsorption by DCT.

homomeric Kir4.1 channels, their maximum activity is reached at a pH_i of approximately 6.5 (18, 19), whereas for heteromeric Kir4.1/Kir5.1, it is reached at pH_i values greater than 7.4. Several SeSAME/EAST mutations in Kir4.1 also shift the pH_i sensitivity of heteromeric Kir4.1/Kir5.1 channels toward an even more alkaline pH, and so the overall effect of these mutations is to reduce channel activity at physiological pH_i values. This is in marked contrast to the effect seen by deletion of the Kir5.1 subunit in these mice because the remaining homomeric Kir4.1 channels in the basolateral membrane possess a reduced pH sensitivity and so display a greater functional activity than that seen in WT *Kir5.1*^{+/+} mice. Small variations in pH_i therefore have the potential to produce major changes in basolateral K⁺ conductance and so we may anticipate that under physiological conditions, changes in pH_i might provide a regulatory link between NaCl uptake in the DCT and the acid/base status by reflecting the extracellular pH, as suggested by early studies (18).

Finally, although we observe a mirror-like phenotype to SeSAME/EAST syndrome in these *Kir5.1*^{-/-} mice, this effect is a result of the complete absence of Kir5.1. In cases in which a stable but dysfunctional Kir5.1 subunit protein is produced, the phenotypic effects are likely to be very different because this subunit would have the potential to act as a dominant-negative subunit downregulating the overall functional activity of the basolateral K⁺ conductance and producing a phenotype more similar to that of SeSAME/EAST. Thus, future studies may reveal a complex range of related tubulopathies caused by mutations in *KCNJ10* and *KCNJ16* with differences being caused by the relative degree of functional activity of the basolateral K⁺ conductance at physiological pH.

Methods

Mice. *Kir5.1*^{-/-} mice were generated as previously described (22). Mutant and WT mice had free access to tap water, and maintained on standard (0.64% K⁺; 0.25% Na⁺) rodent chow (SAFE-A04; Usine d’Alimentation Rationnelle) until the studies began. All animals used in this study were handled in full compliance with the French government welfare policy. This work was performed under Permit 75–096 of the Veterinary Department of the French Ministry of Agriculture.

Paulais et al.

PNAS Early Edition | 5 of 6

Metabolic Studies. *Kir5.1^{+/+}* and *Kir5.1^{-/-}* mice were individually housed in metabolic cages (Techniplast; Usine d'Alimentation Rationnelle), and their body weights, food and water intakes, and urine output were measured daily. Urine was collected under water-saturated mineral oil and in the presence of a few crystals of Thymol (VWR) to prevent bacterial degradation of NH_4^+ . After a 5- to 7-d adaptation period with ad libitum access to water and purified powdered chow (SAFE A210; 0.27% Na^+ , 0.37% K^+ , 0.76% Ca^{2+}), experiments were performed for a period of 5 to 10 d as appropriate. During days 1 to 5 of the experimental period, the mice were kept under control conditions. For the water-restriction experiments, demineralized water was substituted for mains water for 4 to 5 d before the 24-h water-deprivation period.

Methods for urine and blood analysis, immunoblot analysis, and arterial blood pressure measurements are detailed in *SI Methods*.

Diuretic Treatments. Furosemide (Sigma-Aldrich) was given for 6 h at a dose of 90 $\mu\text{g/g}$ body weight/d mixed with the powdered chow. The acute effects of HCTZ (Sigma-Aldrich) on urinary parameters of *Kir5.1^{+/+}* and *Kir5.1^{-/-}* mice was studied 6 h after a single i.p. injection at a dose of 30 $\mu\text{g/g}$ body weight. For chronic treatment, HCTZ was mixed with the powdered chow, and given for 4 d at a dose of 130 $\mu\text{g/g}$ body weight/d (40). Amiloride (Sigma-Aldrich) was dissolved in physiological serum and injected s.c. at a single dose of 1.45 $\mu\text{g/g}$ body weight. Its effects on urinary parameters were measured 6 h after injection.

Electrophysiology. Patch-clamp analysis of single K^+ channels was performed as previously described (6). Briefly, microdissected DCTs were transferred to a physiological saline solution containing (in mM) 140 NaCl, 5 KCl, 1 CaCl_2 , 1 MgCl_2 , 10 glucose, and 10 Hepes, and adjusted to pH 7.4 with NaOH. The

patch pipettes were filled with a high- K^+ solution containing (in mM) 145 KCl, 1 CaCl_2 , 1 MgCl_2 , 10 glucose, and 10 Hepes, and adjusted to pH 7.4 with KOH. When appropriate, the potassium content of pipette solution was reduced to 15 mM by substituting 130 mM NaCl for KCl in the high- K^+ solution. In the cell-excised configuration, the cytoplasmic side of the membrane patch was exposed to a nominally Ca^{2+} - and Mg^{2+} -free solution (6), which contained (in mM) 145 KCl, 5 K-EDTA, 10 glucose, and 10 Hepes, and the pH of which was adjusted to 6.8 to 8 with KOH. Experiments were carried out at room temperature (22–27 °C).

Statistics. All data are reported as means \pm SEM for *n* experiments. Comparisons of parameters between groups were performed with the Mann–Whitney rank-sum test or the Student *t* test for two independent variables. Comparisons of the parameters of two related samples were performed by using the Wilcoxon signed-rank test or Student *t* test for paired variables. *P* values lower than 0.05 were taken to represent statistically significant differences.

ACKNOWLEDGMENTS. We thank Monika Ghosh for help with preparation of the manuscript, and Gregory Messaoudi and Marine Grégoire for contributions during their graduate studies at Université Pierre et Marie Curie Paris 6. We also thank Lijun Shang for help with genotyping, and Sara Wells and the staff at the Mary Lyon Centre, Medical Research Council Harwell, for help with the initial generation and maintenance of the mutant mice. This work was supported by Agence Nationale de la Recherche (ANR) Grant Physio 2007-RPVO7084. M.K. holds a PhD fellowship from the French Ministère de la Recherche. S.K.R. holds a PhD fellowship from the Erasmus Mundus External Cooperation Window Lot 15 India European scholarship program. M.P. is an Institut National de la Santé et de la Recherche Médicale researcher. S.J.T. was supported by the Royal Society.

- Wang W, Hebert SC, Giebisch G (1997) Renal K^+ channels: Structure and function. *Annu Rev Physiol* 59:413–436.
- Lorenz JN, et al. (2002) Impaired renal NaCl absorption in mice lacking the ROMK potassium channel, a model for type II Bartter's syndrome. *J Biol Chem* 277:37871–37880.
- Warth R, et al. (2004) Proximal renal tubular acidosis in TASK2 K^+ channel-deficient mice reveals a mechanism for stabilizing bicarbonate transport. *Proc Natl Acad Sci USA* 101:8215–8220.
- Hurst AM, Duplain M, Lapointe JY (1992) Basolateral membrane potassium channels in rabbit cortical thick ascending limb. *Am J Physiol* 263:F262–F267.
- Paulais M, Lourdel S, Teulon J (2002) Properties of an inwardly rectifying K^+ channel in the basolateral membrane of mouse TAL. *Am J Physiol Renal Physiol* 282:F866–F876.
- Lourdel S, et al. (2002) An inward rectifier K^+ channel at the basolateral membrane of the mouse distal convoluted tubule: Similarities with Kir4-Kir5.1 heteromeric channels. *J Physiol* 538:391–404.
- Taniguchi J, Yoshitomi K, Imai M (1989) K^+ channel currents in basolateral membrane of distal convoluted tubule of rabbit kidney. *Am J Physiol* 256:F246–F254.
- Gray DA, Frindt G, Zhang YY, Palmer LG (2005) Basolateral K^+ conductance in principal cells of rat CCD. *Am J Physiol Renal Physiol* 288:F493–F504.
- Lachheb S, et al. (2008) Kir4.1/Kir5.1 channel forms the major K^+ channel in the basolateral membrane of mouse renal collecting duct principal cells. *Am J Physiol Renal Physiol* 294:F1398–F1407.
- Pessia M, Tucker SJ, Lee K, Bond CT, Adelman JP (1996) Subunit positional effects revealed by novel heteromeric inwardly rectifying K^+ channels. *EMBO J* 15:2980–2987.
- Bockenbauer D, et al. (2009) Epilepsy, ataxia, sensorineural deafness, tubulopathy, and *KCNJ10* mutations. *N Engl J Med* 360:1960–1970.
- Scholl UI, et al. (2009) Seizures, sensorineural deafness, ataxia, mental retardation, and electrolyte imbalance (SeSAME syndrome) caused by mutations in *KCNJ10*. *Proc Natl Acad Sci USA* 106:5842–5847.
- Sala-Rabanal M, Kucheryavykh LY, Skatchkov SN, Eaton MJ, Nichols CG (2010) Molecular mechanisms of EAST/SeSAME syndrome mutations in Kir4.1 (*KCNJ10*). *J Biol Chem* 285:36040–36048.
- Williams DM, et al. (2010) Molecular basis of decreased Kir4.1 function in SeSAME/EAST syndrome. *J Am Soc Nephrol* 21:2117–2129.
- Bandulik S, et al. (2011) The salt-wasting phenotype of EAST syndrome, a disease with multifaceted symptoms linked to the *KCNJ10* K^+ channel. *Pflugers Arch Eur J Physiol* 461:423–435.
- Bond CT, et al. (1994) Cloning and expression of a family of inward rectifier potassium channels. *Receptors Channels* 2:183–191.
- Pessia M, Imbrici P, D'Adamo MC, Salvatore L, Tucker SJ (2001) Differential pH sensitivity of Kir4.1 and Kir4.2 potassium channels and their modulation by heteropolymerisation with Kir5.1. *J Physiol* 532:359–367.
- Tanemoto M, Kittaka N, Inanobe A, Kurachi Y (2000) In vivo formation of a proton-sensitive K^+ channel by heteromeric subunit assembly of Kir5.1 with Kir4.1. *J Physiol* 525:587–592.
- Xu H, Cui N, Yang Z, Qu Z, Jiang C (2000) Modulation of kir4.1 and kir5.1 by hypercapnia and intracellular acidosis. *J Physiol* 524:725–735.
- Tucker SJ, Imbrici P, Salvatore L, D'Adamo MC, Pessia M (2000) pH dependence of the inwardly rectifying potassium channel, Kir5.1, and localization in renal tubular epithelia. *J Biol Chem* 275:16404–16407.
- Yang Z, et al. (2000) Biophysical and molecular mechanisms underlying the modulation of heteromeric Kir4.1-Kir5.1 channels by CO_2 and pH. *J Gen Physiol* 116:33–45.
- D'Adamo MC, et al. (2011) Genetic inactivation of *Kcnj16* identifies Kir5.1 as an important neuronal CO_2 chemoreceptor. *J Biol Chem* 286:192–198.
- Lalioti MD, et al. (2006) Wnk4 controls blood pressure and potassium homeostasis via regulation of mass and activity of the distal convoluted tubule. *Nat Genet* 38:1124–1132.
- Yang SS, et al. (2007) Molecular pathogenesis of pseudohypoaldosteronism type II: generation and analysis of a Wnk4(D561A/+)-knockin mouse model. *Cell Metab* 5:331–344.
- Furgeson SB, Linas S (2010) Mechanisms of type I and type II pseudohypoaldosteronism. *J Am Soc Nephrol* 21:1842–1845.
- Mayan H, et al. (2002) Pseudohypoaldosteronism type II: Marked sensitivity to thiazides, hypercalciuria, normomagnesemia, and low bone mineral density. *J Clin Endocrinol Metab* 87:3248–3254.
- Reichold M, et al. (2010) *KCNJ10* gene mutations causing EAST syndrome (epilepsy, ataxia, sensorineural deafness, and tubulopathy) disrupt channel function. *Proc Natl Acad Sci USA* 107:14490–14495.
- Takumi T, et al. (1995) A novel ATP-dependent inward rectifier potassium channel expressed predominantly in glial cells. *J Biol Chem* 270:16339–16346.
- Yang Z, Jiang C (1999) Opposite effects of pH on open-state probability and single channel conductance of kir4.1 channels. *J Physiol* 520:921–927.
- Kusaka S, et al. (1999) Expression and polarized distribution of an inwardly rectifying K^+ channel, Kir4.1, in rat retinal pigment epithelium. *J Physiol* 520:373–381.
- Tada Y, Horio Y, Kurachi Y (1998) Inwardly rectifying K^+ channel in retinal Müller cells: comparison with the KAB-2/Kir4.1 channel expressed in HEK293T cells. *Jpn J Physiol* 48:71–80.
- Simon DB, et al. (1996) Gitelman's variant of Bartter's syndrome, inherited hypokalaemic alkalosis, is caused by mutations in the thiazide-sensitive Na-Cl cotransporter. *Nat Genet* 12:24–30.
- Nijenhuis T, et al. (2005) Enhanced passive Ca^{2+} reabsorption and reduced Mg^{2+} channel abundance explains thiazide-induced hypocalciuria and hypomagnesemia. *J Clin Invest* 115:1651–1658.
- Nahum H, et al. (1986) Pseudohypoaldosteronism type II: proximal renal tubular acidosis and dDAVP-sensitive renal hyperkalemia. *Am J Nephrol* 6:253–262.
- Ishii M, et al. (1997) Expression and clustered distribution of an inwardly rectifying potassium channel, KAB-2/Kir4.1, on mammalian retinal Müller cell membrane: their regulation by insulin and laminin signals. *J Neurosci* 17:7725–7735.
- Dawson DC, Richards NW (1990) Basolateral K conductance: Role in regulation of NaCl absorption and secretion. *Am J Physiol* 259:C181–C195.
- Mauerer UR, Boulpaep EL, Segal AS (1998) Regulation of an inwardly rectifying ATP-sensitive K^+ channel in the basolateral membrane of renal proximal tubule. *J Gen Physiol* 111:161–180.
- Tsuchiya K, Wang W, Giebisch G, Welling PA (1992) ATP is a coupling modulator of parallel Na,K-ATPase-K-channel activity in the renal proximal tubule. *Proc Natl Acad Sci USA* 89:6418–6422.
- Paulais M, Lachheb S, Teulon J (2006) A Na^+ - and Cl^- -activated K^+ channel in the thick ascending limb of mouse kidney. *J Gen Physiol* 127:205–215.
- Vallet M, et al. (2006) Pendrin regulation in mouse kidney primarily is chloride-dependent. *J Am Soc Nephrol* 17:2153–2163.

Supporting Information

Paulais et al. 10.1073/pnas.1101400108

SI Methods

Urine and Blood Analysis. Freshly collected urine samples obtained from *Kir5.1^{+/+}* and *Kir5.1^{-/-}* mice in the metabolic cages were analyzed for protein content and creatinine, Na⁺, K⁺, Cl⁻, Mg²⁺, Ca²⁺, and PO₄²⁻ concentrations by using a Konelab 20I analyzer (Thermo Fisher Scientific). The urinary ammonium concentration was determined in 1:60 diluted samples according the colorimetric protocol of Berthelot (1), and by absorbance measurements at 623 nm. Urinary pH was measured by using a small-diameter glass pH microelectrode and a 691 pH meter (Metrohm). Urinary aldosterone was measured by a Coat-A-Count aldosterone competitive RIA kit (Diagnostic Products), and values were converted into concentrations according the manufacturer's instructions.

Venous blood from the retroorbital plexus of conscious *Kir5.1^{+/+}* and *Kir5.1^{-/-}* mice was analyzed for pH, hematocrit, gas contents, and concentrations of Na⁺, Ca²⁺ (calculated at pH 7.4), and Cl⁻ by a ABL77 blood gas analyzer (Radiometer). Plasma creatinine, osmolality, and K⁺ were measured from blood samples taken from the tail artery or at the time the animals were killed. Blood K⁺ was measured by using the ABL77 analyzer, and plasma creatinine levels were measured by a Dionex BX-500 high-pressure liquid ion chromatograph (Dionex) according to a previously described method (2) and converted into concentrations by using an external standard curve. Urine and plasma osmolalities were measured by an Autocal 13DR freezing point osmometer (Hermann Roebling) after 1:10 or 1:20 dilution of the samples as appropriate. Whole kidney filtration rates, fractional excretions of ions, blood and urine anion gaps, and blood bicarbonates were calculated from the values measured.

At the end of the experimental period, the animals were killed after anesthetizing by the peritoneal injection of ketamine and

xylazine (0.1 and 0.01 mg/g body weight, respectively). Blood was collected on heparin, and the kidneys were removed.

Immunoblot Analysis. *Kir5.1^{+/+}* and *Kir5.1^{-/-}* mice were anesthetized by peritoneal injection of ketamine and xylazine (0.1 and 0.01 mg/g body weight, respectively) and killed by cervical dislocation. The kidneys were rapidly removed and washed in ice-cold buffer, and the medullary tissue was discarded. Membrane fraction preparation and immunoblotting procedures for comparing two sets of samples of renal cortical membranes with regard to the relative abundance of specific proteins were as described (3, 4). Coomassie-stained polyacrylamide gels were used to check that equal quantities of protein were loaded for each series. The dilutions of primary antibodies were as follows: anti-NKCC2, 1:10,000; anti- α -ENaC, 1:10000; anti-NCC, 1:30,000; and anti-NHE3 1:5,000. Densitometric values for *Kir5.1^{-/-}* mice were normalized to the mean for *Kir5.1^{+/+}* mice, which was defined as 100%, and results were expressed as means \pm SEM.

Arterial Blood Pressure. Systolic blood pressure was measured in conscious mice by using a BP-2000 blood pressure analysis tail cuff system (Visitech Systems). Variability in testing conditions was minimized by measuring all mice of a given strain at the same time. For each mouse, 10 measurements were repeated over a period of 3 d for acclimatization purposes, and data were discarded. Test measurements were performed over the next 2 d. Systolic blood pressure values lower than 80 mm Hg on individual test measurements, which were probably attributable to a pulse-detection failure, were discarded. The systolic blood pressure from the remaining individual test measurements were averaged, and taken as the blood pressure for each mouse.

1. Berthelot MPE (1859) Violet d'aniline. *Repert Chim Appl* 1:284.
2. Dunn SR, Qi Z, Bottinger EP, Breyer MD, Sharma K (2004) Utility of endogenous creatinine clearance as a measure of renal function in mice. *Kidney Int* 65:1959–1967.
3. Quentin F, et al. (2004) The Cl⁻/HCO₃⁻ exchanger pendrin in the rat kidney is regulated in response to chronic alterations in chloride balance. *Am J Physiol Renal Physiol* 287: F1179–F1188.

4. Quentin F, et al. (2004) Regulation of the Cl⁻/HCO₃⁻ exchanger AE2 in rat thick ascending limb of Henle's loop in response to changes in acid-base and sodium balance. *J Am Soc Nephrol* 15:2988–2997.

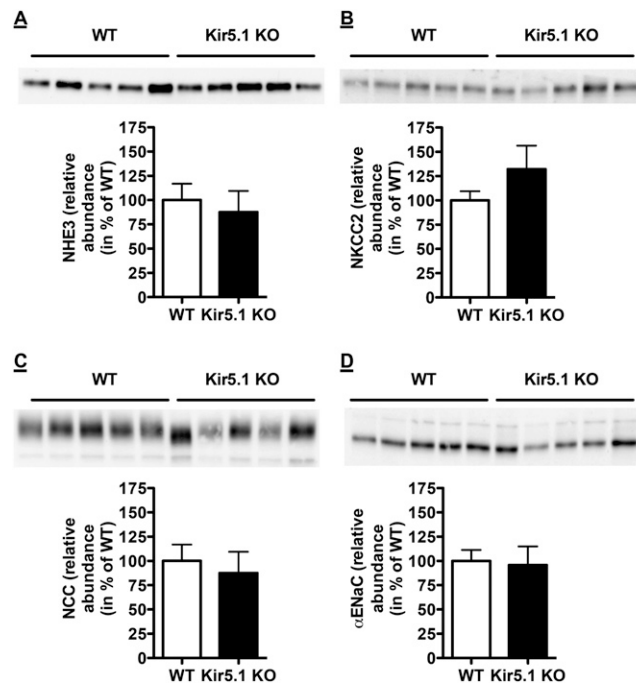


Fig. S1. Semiquantitative immunoblotting of membrane fractions from cortex dissected from *Kir5.1*^{+/+} and *Kir5.1*^{-/-} mice kidneys. Immunoblots of samples from *Kir5.1*^{+/+} ($n = 5$) and *Kir5.1*^{-/-} ($n = 5$) mice incubated with (A) anti-Na/H exchanger (NHE3) antibody showing a distinct band at approximately 87 kDa, with (B) anti-NaK2Cl cotransporter (NKCC2) showing a distinct band at 160 to 170 kDa, with (C) anti-NCC showing a distinct band at approximately 130 kDa, and with (D) anti- α ENaC antibody showing a distinct band at approximately 100 kDa. Densitometric analysis showed that the abundance (means \pm SEM) of NHE3, NKCC2, NCC, and α ENaC in *Kir5.1*^{-/-} mice (filled bars) were not different compared with *Kir5.1*^{+/+} mice (open bars).

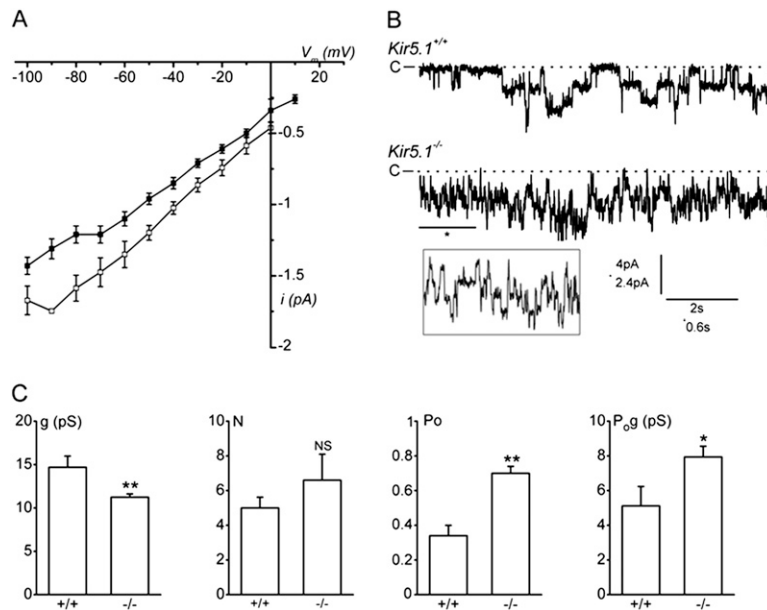


Fig. S2. K^+ currents in the basolateral membrane of DCT tubules with 15 mM K^+ in the pipette. (A) Current (i)–voltage (V_m) relationships for K^+ channels recorded in the DCTs of *Kir5.1*^{+/+} (□) and *Kir5.1*^{-/-} (■) mice in the cell-attached configuration. Tubules were bathed with physiological saline solution, and the pipette contained 15 mM KCl. Values are means of seven and 10 patches from *Kir5.1*^{+/+} mice and *Kir5.1*^{-/-} mice, respectively. Error bars represent SEM when larger than symbols. (B) Current traces recorded in the cell-attached mode at a clamped potential of -60 mV. "C" indicates the closed current level. The expanded inset trace corresponds to the segment of recordings in *Kir5.1*^{-/-} mice indicated by the asterisk. (C) Diagrams for the single-channel conductances (g), the number of channels per patch (N), the P_o , and the averaged unit conductance ($P_o \cdot g$) for the two groups of mice. Values are means of the numbers patches in *Kir5.1*^{+/+} and *Kir5.1*^{-/-} mice given in A. Error bars represent SEM; ** $P < 0.01$ and * $P < 0.05$; NS, no significant difference.

